

High-Speed and High-Quality Text-to-Lip Generation

Jinglin Liu*

Zhejiang University

jinglinliu@zju.edu.cn

Zhiying Zhu*

Zhejiang University

zhyi0625@gmail.com

Yi Ren*

Zhejiang University

rayeren@zju.edu.cn

Zhou Zhao

Zhejiang University

zhaozhou@zju.edu.cn

Abstract

As a key component of talking face generation, lip movements generation determines the naturalness and coherence of the generated talking face video. Prior literature mainly focuses on speech-to-lip generation while there is a paucity in text-to-lip (T2L) generation. T2L is a challenging task and existing end-to-end works depend on the attention mechanism and autoregressive (AR) decoding manner. However, the AR decoding manner generates current lip frame conditioned on frames generated previously, which inherently hinders the inference speed, and also has a detrimental effect on the quality of generated lip frames due to error propagation. This encourages the research of parallel T2L generation. In this work, we propose a novel parallel decoding model for high-speed and high-quality text-to-lip generation (HH-T2L). Specifically, we predict the duration of the encoded linguistic features and model the target lip frames conditioned on the encoded linguistic features with their duration in a non-autoregressive manner. Furthermore, we incorporate the structural similarity index loss and adversarial learning to improve perceptual quality of generated lip frames and alleviate the blurry prediction problem. Extensive experiments conducted on GRID and TCD-TIMIT datasets show that 1) HH-T2L generates lip movements with competitive quality compared with the state-of-the-art AR T2L model DualLip and exceeds the baseline AR model TransformerT2L by a notable margin benefiting from the mitigation of the error propagation problem; and 2) exhibits distinct superiority in inference speed (an average speedup of $19\times$ than DualLip on TCD-TIMIT).¹

1. Introduction

In the modern service industries, talking face generation has broad application prospects such as avatar, virtual assistant, movie animation, teleconferencing, etc. [47, 7]. As a key component of talking face generation, lip movements

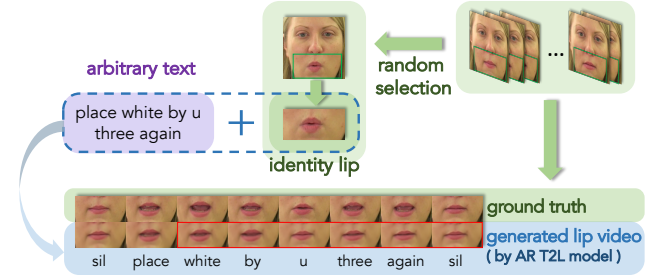


Figure 1: The task description of T2L generation. The model takes in an arbitrary source text sequence and a single identity lip image to synthesize the target lip movements video. And in this figure we can see that the generated video loses the linguistic information gradually and finally becomes fuzzy and motionless (lip frames in the red box), which is the intractable problem existing in AR T2L models due to error propagation.

generation (a.k.a. lip generation) determines the naturalness and coherence of the generated talking face video. Lip generation aims to synthesize accurate mouth movements video corresponding to the linguistic content information carried in speech or pure text.

Mainstream literature focuses on speech-to-lip (S2L) generation while there is a paucity in text-to-lip (T2L) generation. Even so, T2L generation is very crucial and has considerable merits compared to S2L since 1) text data can be obtained or edited more easily than speech, which makes T2L generation more convenient; and 2) T2L extremely preserves privacy especially in the society where the deep learning techniques are so developed that a single sentence speech could expose an unimaginable amount of personal information.

However, end-to-end T2L task (shown in Figure 1) is challenging. Unlike S2L task where the mapping relationship between the sequence length of source speech and target video is certain (according to audio sample rate and fps), there is an uncertain sequence length discrepancy between source and target in T2L task. The traditional temporal convolutional networks become impractical. Hence, existing

¹* equal contribution.

works view T2L as a sequence-to-sequence task and tackle it by leveraging the attention mechanism and autoregressive (AR) decoding manner. The AR decoding manner brings two drawbacks: 1) it inherently hinders the inference speed since its decoder generates target lips one by one autoregressively with the causal structure. Consequently, generating a single sentence of short video consumes about 0.5-1.5 seconds even on GPU, which is not acceptable for industrial applications such as real-time interactions with avatar or virtual assistant, real-time teleconferencing and document-level audio-visual speech synthesis, etc. 2) It has a detrimental effect on the quality of generated lips due to error propagation², which is frequently discussed in neural machine translation and image caption field [4, 41]. Worse still, error propagation is more obvious in AR lip generation than in other tasks, because the mistakes could take place at more dimensions (every pixel with three channels in generated image) and there is information loss during the down-sampling when sending the last generated lip frame to predict current one. Although prior work DualLip [7] alleviates the error propagation by incorporating the technique of location-sensitive attention, it still has an unsatisfying performance on long-sequence datasets due to accumulated prediction error.

To address such limitations, we turn to non-autoregressive (NAR) approaches. NAR decoding manner generates all the target tokens in parallel, which has already pervaded multiple research fields such as neural machine translation [17, 23, 16, 25], speech recognition [6, 19], speech synthesis [31, 29, 28], image captioning [11] and lip reading [24]. These works utilize the NAR decoding in sequence-to-sequence tasks to reduce the inference latency or generate length-controllable sequence.

In this work, we propose an NAR model for high-speed and high-quality T2L generation (HH-T2L). HH-T2L predicts the duration of the encoded linguistic features and model the target lip frames conditioned on the encoded linguistic features with their duration in a non-autoregressive manner. Further, we leverage structural similarity index (SSIM) loss to supervise HH-T2L generating lips with better perceptual quality. Finally, using only reconstruction loss and SSIM loss is insufficient to generate distinct lip images with more realistic texture and local details (*e.g.* wrinkles, beard and teeth), and therefore we adopt adversarial learning to mitigate this problem.

Our main contributions can be summarized as follows: 1) We point out and analyze the unacceptable inference latency and intractable error propagation existing in AR T2L generation. 2) To circumvent these problems, we propose a novel parallel decoding model HH-T2L to generate high-

quality lips with low inference latency. And as a byproduct of HH-T2L, the duration predictor in HH-T2L could be leveraged in an NAR text-to-speech model, which naturally enables the synchronization in audio-visual speech synthesis task. 3) Extensive experiments demonstrate that HH-T2L generates the competitive lip movements quality compared with state-of-the-art AR T2L model DualLip and exceeds the baseline AR model TransformerT2L by a notable margin. In the meanwhile, HH-T2L exhibits distinct superiority in inference speed (19× average speedup than DualLip on TCD-TIMIT), which truly provides the possibility to bring T2L generation from laboratory to industrial applications.

2. Related Work

2.1. Talking Face Generation

Talking face generation aims to generate realistic talking face video and covers many applications such as avatar and movie animation. There is a branch of works in computer graphics (CG) field exploring it [39, 13, 35, 42, 1] through hidden Markov models or deep neural network. These works synthesize the whole face by generating the intermediate parameters, which can then be used to deform a 3D face. Thanks to the evolved convolutional neural network (CNN) and high-performance computing resources, end-to-end systems which synthesize 2D talking face images by CNN rather than rendering methods in CG, have been presented recently in the computer vision (CV) field [22, 8, 5, 37, 46, 47, 45, 7, 30]. Most of them focus on synthesizing lip movements images and then transforming them to faces. We mainly take these works in CV field into consideration and broadly divide them into two streams as the following paragraphs.

Speech-to-Lip Generation Previous speech-driven works *e.g.* [8] simply generate the talking face images conditioned on the encoded speech and the encoded face image carrying the identity information. To synthesize more accurate and distinct lip movements, Chen *et al.* [5] introduce the task of speech-to-lip generation using lip image as the identity information. Further, Song *et al.* [33] add a lip-reading discriminator to focus on the mouth region, and Zhu *et al.* [47] add the dynamic attention on lip area to synthesize talking face while keeping the lip movements realistic. Prajwal *et al.* [30] propose a pre-trained lip-syncing discriminator to synthesize talking face with speech-consistent lip movements.

Text-to-Lip Generation The literature of direct text-to-lip generation is rare. Some text-driven approaches either cascade the text-to-speech and speech-to-lip generation

²Error propagation means if a token is mistakenly predicted at inference stage, the error will be propagated and the future tokens conditioned on this one will be influenced [4, 41].

model [21, 22], or combine the text feature with speech feature together to synthesize lip movements [43]. Fried *et al.* [14] edit a given video based on pure speech-aligned text sequence. Unlike the scenario where source speech or video is given, the sequence length of target lip frames is uncertain with only text input. Existing work [7] depends on the attention mechanism and AR decoding method to generate the target lip frames until the stop token is predicted.

2.2. Non-Autoregressive Sequence Generation

In sequence-to-sequence tasks, an autoregressive (AR) model takes in a source sequence and then generates tokens of the target sentence one by one with the causal structure at inference [34, 36]. Since the AR decoding manner causes the high inference latency, many non-autoregressive (NAR) models, which generate target tokens conditionally independent of each other, have been proposed recently. Earliest in the NAR machine translation field, many works use the fertility module or length predictor [17, 23, 16, 25] to predict the length correspondence (fertility) between source and target sequences, and then generate the target sequence depending on the source sequence and predicted fertility. Shortly afterward, researchers bring NAR decoding manner into heterogeneous tasks. In the speech field, NAR-based TTS [31, 29, 28] synthesize speech from text with high speed and slightly quality drop; NAR-based ASR [6, 19] recognize speech to corresponding transcription faster. In the computer vision field, Liu *et al.* [24] propose an NAR model for lipreading; Deng *et al.* [11] present NAR image caption model not only improving the decoding efficiency but also making the generated captions more controllable and diverse.

3. Method

In this section, we first introduce the preliminary knowledge of text-to-lip generation problem, and then explain each module in HH-T2L model thoroughly. Finally, we describe the methods which HH-T2L leverages to further improve the generated video quality.

3.1. Preliminary Knowledge

The text-to-lip generation aims to generate the sequence of lip movement video frames $\mathcal{L} = \{l_1, l_2, \dots, l_T\}$, given source text sequence $\mathcal{S} = \{s_1, s_2, \dots, s_m\}$ and a single identity lip image l_I as condition. Generally, there is considerable discrepancy between the sequence length of \mathcal{L} and \mathcal{S} with uncertain mapping relationship. Previous work [7] views this as a sequence-to-sequence problem, utilizing attention mechanism and AR decoding manner, where the conditional probability of \mathcal{L} can be formulated as:

$$P(\mathcal{L}|\mathcal{S}, l_I) = \prod_{\tau=0}^T P(l_{\tau+1}|l_{<\tau+1}, \mathcal{S}, l_I; \theta), \quad (1)$$

where θ denotes the parameters of the model.

To remedy the error propagation and high latency problem brought by AR decoding, HH-T2L models the target sequence in an NAR manner, where the conditional probability becomes:

$$P(\mathcal{L}|\mathcal{S}, l_I) = \prod_{\tau=1}^T P(l_{\tau}|\mathcal{S}, l_I; \theta). \quad (2)$$

3.2. Model Architecture of HH-T2L

The overall model architecture and training losses are shown in Figure 2a. We explain each component in HH-T2L in the following paragraphs.

Identity Encoder As shown in the right panel of Figure 2a, identity encoder consists of stacked 2D convolutional layers with batch normalization, which down-samples the identity image multiple times to extract features. The identity image is selected randomly from target lip frames, providing the appearance information of a speaker. It is worth noting that the identity encoder sends out the final encoded hidden feature together with the intermediate hidden feature of convolutional layers at every level, which provides the fine-grained image information.

Text Encoder As shown in Figure 2b, the text encoder consists of a text embedding layer, stacked feed-forward Transformer layers (FFT) [31], a duration predictor and a length regulator. The FFT layer contains self-attention layer and 1D convolutional layer with layer normalization and residual connection [36, 15]. The duration predictor contains two 1D convolutional layers with layer normalization and one linear layer, which takes in the hidden text embedding sequence and predicts duration sequence $\mathcal{D}^* = \{d_1^*, d_2^*, \dots, d_m^*\}$, where d_i^* means how many video frames the i -th text token corresponding to. The length regulator expands the hidden text embedding sequence according to ground truth duration \mathcal{D} at training stage or predicted duration \mathcal{D}^* at inference stage. For example, when given source text and duration sequence are $\{s_1, s_2, s_3\}$ and $\{2, 1, 3\}$ respectively, denoting the hidden text embedding as $\{h_1, h_2, h_3\}$, the expanded sequence is $\{h_1, h_1, h_2, h_3, h_3, h_3\}$, which carries the linguistic information corresponding to lip movement video at frame level. Collectively, text encoder encodes the source text sequence \mathcal{S} to linguistic information sequence $\tilde{\mathcal{S}} = \{\tilde{s}_1, \tilde{s}_2, \dots, \tilde{s}_{T^*}\}$, where $T^* = \sum_{i=1}^m d_i$ at training stage, or $T^* = \sum_{i=1}^m d_i^*$ at inference stage.

Motion Decoder Motion decoder (Figure 2c) aims to model the lip movement information sequence $\tilde{\mathcal{L}} = \{\tilde{l}_1, \tilde{l}_2, \dots, \tilde{l}_{T^*}\}$ from linguistic information sequence $\tilde{\mathcal{S}}$. It

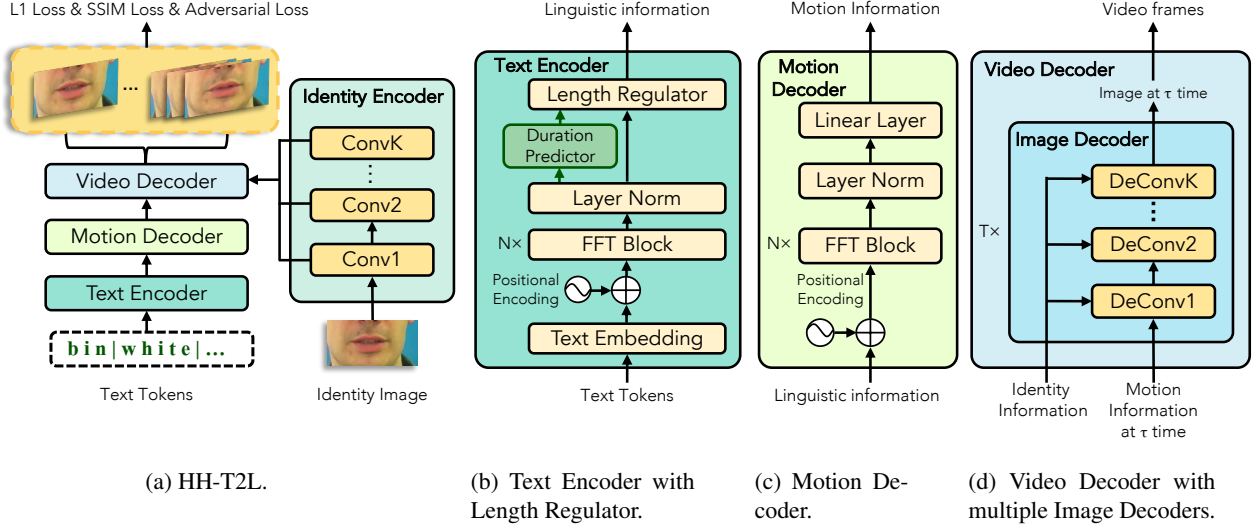


Figure 2: The overall architecture for HH-T2L. In subfigure (a), Identity Encoder sends out residual information at every convolutional layer. In subfigure (b), Length Regulator expands the text sequence according to ground truth duration in training or predicted duration in inference. In subfigure (c), Motion Decoder models lip movement information sequence from linguistic information sequence. In subfigure (d), there are T Image Decoders placed parallel in Video Decoder. The τ -th Image Decoder takes in motion information at τ time and generates lip image at τ time. T means total number of lip frames.

utilizes the positional encoding and self-attention mechanism in stacked FFT blocks to enforce the temporal correlation on the hidden sequence. There is a linear layer at the end of this module convert the hidden states to an appropriate dimension.

Video Decoder The video decoder generates the target lip movement video \mathcal{L}^* conditioned on the motion information sequence and identity information. As shown in Figure 2d, the video decoder consists of multiple parallel image decoders with all parameters shared, each of which contains stacked 2D deconvolutional layers, and there are skip connections at every level between the identity encoder and each image decoder. The skip connection is implemented by concatenation. Then two extra 2D convolutional layers are added at the end of each decoder for spatial coherence. Finally, the τ -th image decoder takes in lip motion information at τ time \tilde{l}_τ and generates lip image l_τ^* at τ time in corresponding shape.

3.3. Training Methods

In this section, we describe the loss function and training strategy to supervise HH-T2L. The reconstruction loss and duration prediction loss endow the model with the fundamental ability to generate lip movement video. To generate the lip with better perceptual quality and alleviate the “blurry predictions” [27] problem, the structural similarity index loss and adversarial learning are introduced.

Reconstruction Loss Basically, we optimize the whole network by adding L_1 reconstruction loss on generated lip sequence \mathcal{L}^* :

$$L_{rec} = \sum_{\tau=1}^T \|l_\tau - l_\tau^*\|_1 \quad (3)$$

Duration Prediction Loss In the training stage, we add L_1 loss on predicted duration sequence \mathcal{D}^* at token level³ and sequence level, which supervises the duration predictor to make the precise fine-grained and coarse-grained predictions. Duration prediction loss L_{dur} can be written as:

$$L_{dur} = \sum_{i=1}^m \|d_i - d_i^*\|_1 + \left\| \sum_{i=1}^m d_i - \sum_{i=1}^m d_i^* \right\|_1 \quad (4)$$

Structural Similarity Index Loss Structural Similarity Index (SSIM) [40] is adopted to measure the perceptual image quality, which takes luminance, contrast and structure into account, and is close to the perception of human beings. The SSIM value for two pixels at position (i, j) in τ -th images l_τ^* and l_τ can be formulated as:

$$SSIM_{i,j,\tau} = \frac{2\mu_{l_\tau^*}\mu_{l_\tau} + C_1}{\mu_{l_\tau^*}^2 + \mu_{l_\tau}^2 + C_1} \cdot \frac{2\sigma_{l_\tau^*}l_\tau + C_2}{\sigma_{l_\tau^*}^2 + \sigma_{l_\tau}^2 + C_2},$$

³Character level for GRID and phoneme level for TCD-TIMIT following Chen *et al.* [7].

where $\mu_{l_\tau^*}$ and μ_{l_τ} denotes the mean for regions in image l_τ^* and l_τ within a 2D-window surrounding (i, j) . Similar, $\sigma_{l_\tau^*}$ and σ_{l_τ} are standard deviation; $\sigma_{l_\tau^* l_\tau}$ is the covariance; C_1 and C_2 are constant values. To improve the perceptual quality of the generated lip frames, we leverage SSIM loss in HH-T2L. Assuming the size of each lip frame to be $(A \times B)$, the SSIM loss between generated \mathcal{L}^* and ground truth \mathcal{L} becomes:

$$L_{ssim} = \frac{1}{T \cdot A \cdot B} \sum_{\tau=1}^T \sum_i^A \sum_j^B (1 - SSIM_{i,j,\tau}). \quad (5)$$

Adversarial Learning Through experiments, it can be found that only using above losses is insufficient to generate distinct lip images with more realistic texture and local details (e.g. wrinkles, beard and teeth). Thus, we adopt adversarial learning to mitigate this problem and train a quality discriminator *Disc* along with HH-T2L. The *Disc* contains stacked 2D convolutional layers with LeakyReLU activation which down-samples each image to $1 \times 1 \times H$ (H is hidden size), and a 1×1 convolutional layer to project the hidden states to a value of probability for judging real or fake. We use the loss function in LSGAN [26] to train HH-T2L and *Disc*:

$$L_{adv}^G = \mathbb{E}_{x \sim l^*} (Disc(x) - 1)^2, \quad (6)$$

$$L_{adv}^D = \mathbb{E}_{x \sim l} (Disc(x) - 1)^2 + \mathbb{E}_{x \sim l^*} Disc(x)^2, \quad (7)$$

where l^* means lip images generated by HH-T2L and l means ground truth lip images.

To summarize, we optimize the *Disc* by minimizing Equation 7, and optimize the HH-T2L by minimizing L_{total} :

$$L_{total} = \lambda_1 \cdot L_{rec} + \lambda_2 \cdot L_{dur} + \lambda_3 \cdot L_{ssim} + \lambda_4 \cdot L_{adv}^G, \quad (8)$$

where the λ_1 , λ_2 , λ_3 and λ_4 are hyperparameters to trade off the four losses.

4. Experimental Settings

4.1. Datasets

GRID The GRID dataset [10] consists of 33 video-available speakers, and each speaker utters 1,000 phrases. The phrases are in a 6-categories structure following fixed simple grammar: *command*⁴ + *color*⁴ + *preposition*⁴ + *letter*²⁵ + *digit*¹⁰ + *adverb*⁴ where the number denotes how many choices of each category. Thus, the total vocabulary size is 51, composing 64,000 possible phrases. All the videos last 3 seconds with frame rate 25 fps, which form a total duration of 27.5 hours. It is a typical talking face dataset and there are a considerable of lip-related works [3, 38, 9, 2, 5, 47, 7] conducting experiments on it. Following Assael *et al.* [3, 7], we select 255 random samples from each speaker to form the test set.

TCD-TIMIT The TCD-TIMIT dataset [18] is closer to real cases and more challenging than GRID dataset, since 1) the vocabulary is not limited; 2) the sequence length of videos is not fixed and is longer than that in GRID. We use the ‘volunteers’ subset of TCD-TIMIT following Chen *et al.* [7], which consists of 59 speakers uttering about 98 sentences individually. The frame rate is 29.97 fps and each video lasts 2.5~8.1 seconds. The total duration is about 7.5 hours. We set 30% of data from each speaker aside for testing following the recommended speaker-dependent train-test splits [18].

4.2. Data Pre-processing

As for the video pre-processing, we utilize Dlib [20] to detect 68 facial landmarks (including 20 mouth landmarks), and extract the face images from video frames. We resize the face images to 256×256 , and further crop each face to a fixed 160×80 size containing the lip-centered region. As for the text pre-processing, we encode the text sequence at the character level for GRID dataset and phoneme level for TCD-TIMIT dataset following [18, 7]. And when it comes to ground truth duration extraction, we first extract the speech audio from video files, and then utilize ‘Penn Phonetics Lab Forced Aligner’ (P2FA) [44] to get speech-to-text alignments, from which we obtain the duration of each text token for training our duration predictor in HH-T2L.

4.3. Implementation Detail

In our framework, for the FFT blocks, we adopt Transformer [36] as the basic structure. Thereinto, the model hidden size d_{hidden} , number of stacked layers n_{FFT} , number of attention heads n_{head} and dropout rate are set to 256, 4, 2, and 0.2 respectively. For the convolutional layers, the number of stacked layers and kernel size are set to 4 and 5 by default. The window size for calculating SSIM is set to 11. As for the identity lip image, we randomly select an identity lip from target lip frames at training stage, and use the first lip frame at inference stage.

To train HH-T2L, the weights of loss functions λ_1 , λ_2 , λ_3 and λ_4 are set to 1, 1, 1 and 5. The batch size is set to 4 and the total number of iterations is set to 110,000. The learning rate is set as 0.001 and 0.0001 for generator and discriminator respectively using Adam optimizer. The training is run on one RTX 2080ti GPU and our implementation is based on Pytorch Lightning [12]. We will release our code once the paper is published.

4.4. Evaluation Metrics

Following previous T2L generation work [7], we adopt PSNR, SSIM [40] and Landmark Distance (LMD) [5, 33, 7] for quantitative evaluation of lip quality. PSNR and SSIM are the classical reconstruction metrics to evaluate the im-

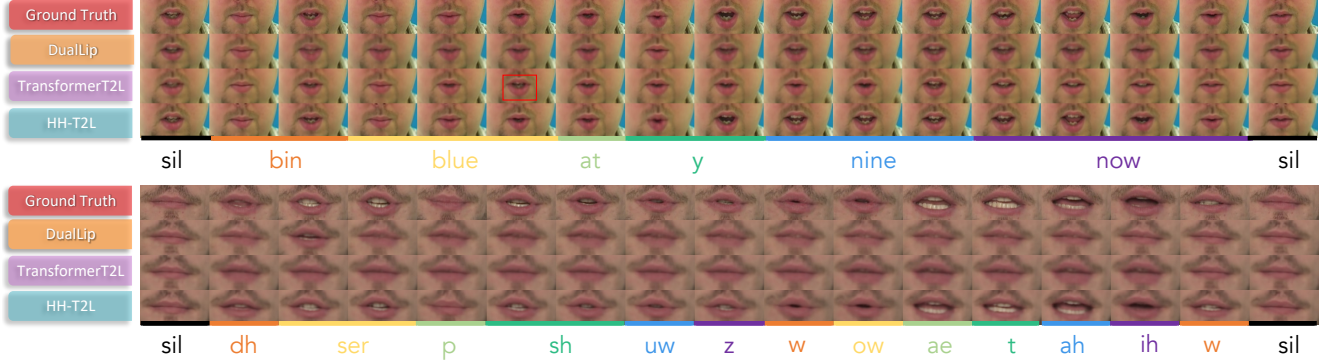


Figure 3: The qualitative comparison among AR SOTA (*DualLip*), AR baseline (*TransformerT2L*) and our NAR method (*HH-T2L*). We visualize two cases from GRID dataset and TCD-TIMIT dataset to illustrate the error propagation problem existing in AR generation and verify the robustness of *HH-T2L*. In the first case, the lip sequence generated from AR baseline predicts a wrong lip image (the 6-th frame with red box), and as a result, the subsequent lip images conditioned on that image becomes out of synchronization with linguistic information and ends in chaos; *DualLip* alleviates the error propagation to some degree. In the second case, both AR models perform poorly on the long-sequence dataset and generate the frames that look speechless as the time goes further.

ages quality in generated video [27]. LMD measures lip movement accuracy from pixel-level [33]. Following Chen *et al.* [7], we calculate the euclidean distance between corresponding lip landmarks of the generated lip movements and ground truth, instead of all the facial landmarks.

5. Results and Analysis

In this section, we present extensive experimental results to evaluate the performance of *HH-T2L* in terms of lip movements quality and inference speedup. And then, we conduct ablation experiments to verify the significance of all proposed methods in *HH-T2L*.

5.1. Quality Comparison

We compare our model with 1) *DualLip* [7], which is the state-of-the-art (SOTA) autoregressive text-to-lip model based on RNN and location sensitive attention [32]. And 2) *TransformerT2L*, an autoregressive baseline model based on Transformer [36] implemented by us, which uses the same model settings with *HH-T2L*⁴, for the sake of fair comparison on both quality and inference speed. The quantitative results on GRID and TCD-TIMIT are listed in Table 1 and Table 2 respectively⁵. Reported results are all in the optimal configuration of each method.⁶

⁴Most modules and the total number of model parameters in *HH-T2L* and *TransformerT2L* are similar.

⁵Note that the reported results are all under the case where the ground truth duration is not provided at inference (denoted as w/o duration [7]), since there is no ground truth duration available in the real case.

⁶For the qualitative evaluation, we put more demos in the supplementary material.

Methods	PSNR \uparrow	SSIM \uparrow	LMD \downarrow
AR Benchmarks			
<i>DualLip</i>	29.13 [†]	0.872 [†]	1.809 [†]
<i>TransformerT2L</i>	26.85	0.829	1.980
Our Model			
<i>HH-T2L</i>	28.74	0.875	1.675

Table 1: Comparison with Autoregressive Benchmarks on GRID dataset. [†] denotes our reproduction under the case w/o ground truth duration at inference.

Methods	PSNR \uparrow	SSIM \uparrow	LMD \downarrow
AR Benchmarks			
<i>DualLip</i>	27.38 [†]	0.809 [†]	2.351 [†]
<i>TransformerT2L</i>	26.89	0.794	2.763
Our Model			
<i>HH-T2L</i>	27.64	0.816	2.084

Table 2: Comparison with Autoregressive Benchmarks on TCD-TIMIT dataset. [†] denotes our reproduction under the case w/o ground truth duration at inference.

5.1.1 Quantitative Comparison

We can see that: 1) On GRID dataset (Table 1), *HH-T2L* outperforms *DualLip* on LMD metric, and keeps the same performance with *DualLip* in terms of PSNR and SSIM metrics. However, on TCD-TIMIT dataset (Table 2), *HH-T2L* achieves a overall performance surpassing *Dual-*

Lip by a notable margin, since autoregressive models perform badly on the long-sequence dataset due to accumulated prediction error. We also visualize this phenomenon in Figure 4; 2) *HH-T2L* shows absolute superiority over AR baseline *TransformerT2L* in terms of three quantitative metrics on both datasets; 3) Although *DualLip* outperforms AR baseline by incorporating the technique of location-sensitive attention, which could alleviate the error propagation, it is still vulnerable on long-sequence dataset.

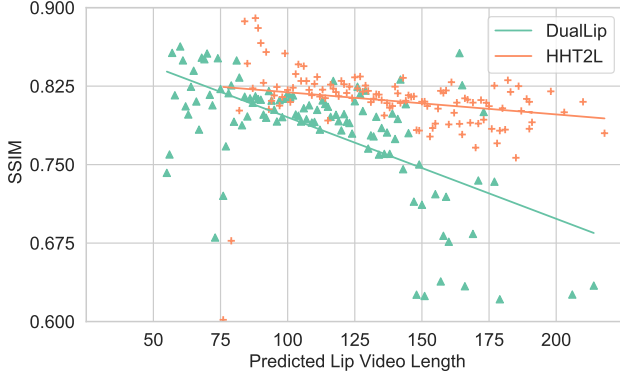


Figure 4: Relationship between SSIM metric and predicted video length for *DualLip* and *HH-T2L* on TCD-TIMIT dataset.

5.1.2 Qualitative Comparison

We further visualize the qualitative comparison between *DualLip*, *TransformerT2L* and *HH-T2L* in Figure 3. It can be seen that the quality of lip frames generated by *DualLip* and *TransformerT2L* become increasingly worse as the time goes further. Concretely, The lip image becomes fuzzy and out of synchronization with linguistic contents. We attribute this phenomenon to the reason that: error propagation problem is serious in AR T2L since the wrong prediction could take place at more dimensions (every pixel with three channels in generated image) and there is information loss during the down-sampling when sending the last generated lip frame to predict current one. What’s worse, on TCD-TIMIT, a long-sequence dataset, *DualLip* and *TransformerT2L* often generate totally unsatisfying results that look like speechless video. By contrast, the lip frames generated by NAR model *HH-T2L* maintain high fidelity to ground truth all the while, which demonstrates the effectiveness and robustness of NAR decoding.

5.2. Speed comparison

In this section, we evaluate and compare the average inference latency of *DualLip*, *TransformerT2L* and *HH-T2L*

on both datasets. Further, we study the relationship between inference latency and the target video length.

5.2.1 Comparison of Average Inference Latency

The average inference latency is the average time consumed to generate one video sample on the test set, which is measured in seconds. Table 3 exhibits the inference latency of *DualLip*, *TransformerT2L* and *HH-T2L*, and the speedup relative to *DualLip*. It can be found that, 1) compared with *DualLip*, *HH-T2L* speeds up the inference by $13.09\times$ and $19.12\times$ on average on two datasets; 2) *TransformerT2L* has the same structure with *HH-T2L*, but runs about 50% slower than *DualLip*, which proves that it is NAR decoding manner in *HH-T2L* speeds up the inference, rather than the modification of model structure; 3) In regard to AR models, the time consumption of a single sentence increases to 0.5-1.5 seconds even on GPU, which is unacceptable for real-world application. By contrast, *HH-T2L* addresses the inference latency problem satisfactorily.

Datasets	Methods	Latency (s)	Speedup
GRID	<i>DualLip</i>	0.299	$1.00\times$
	<i>TransformerT2L</i>	0.689	$0.43\times$
	<i>HH-T2L</i>	0.022	$13.09\times$
TIMIT	<i>DualLip</i>	0.650	$1.00\times$
	<i>TransformerT2L</i>	1.278	$0.51\times$
	<i>HH-T2L</i>	0.034	$19.12\times$

Table 3: The comparison of inference latency on GRID and TCD-TIMIT dataset. The computations are conducted on a server with 1 NVIDIA 2080Ti GPU, 40 Intel Xeon CPUs. The batch size is set to 1. The average length of the generated lip movement sequence is 75 on GRID, and 137 on TCD-TIMIT dataset.

5.2.2 Relationship between Inference Latency and Video Length

In this section, we visualize the relationship between inference latency and sequence length for *DualLip*, *TransformerT2L* and *HH-T2L* respectively, and then study the speedup as the sequence length increases. The experiment is conducted on TCD-TIMIT, since its videos are not in a fixed length. From Figure 5, it can be seen that 1) *HH-T2L* model speeds up the inference obviously due to high parallelization compared with AR models; 2) *HH-T2L* is insensitive to sequence length and almost holds a constant inference latency, but by contrast, the inference latency of *DualLip* and *TransformerT2L* increase linearly as the sequence length increases. As a result, the speedup of *HH-T2L* rel-

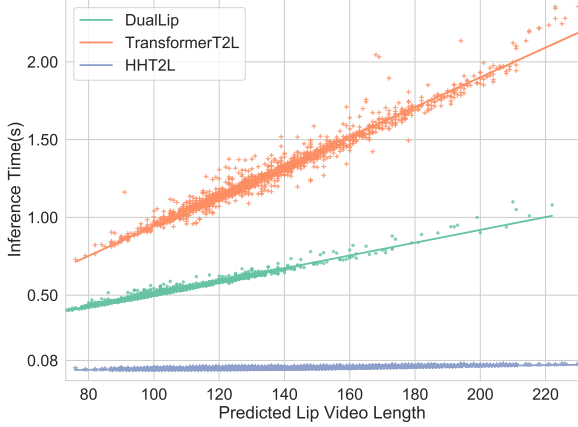


Figure 5: Relationship between inference latency (seconds) and predicted video length for *DualLip*, *TransformerT2L* and *HH-T2L*.

ative to *DualLip* or *TransformerT2L* also increases linearly as the sequence length increases.

5.3. Ablation Study

Model	PSNR \uparrow	SSIM \uparrow	LMD \downarrow	FID \downarrow
Base model	30.24	0.896	0.998	56.36
+SSIM	<u>30.51</u>	<u>0.906</u>	<u>0.978</u>	55.05
+ADV	25.70	0.736	2.460	65.88
+SSIM+ADV	28.36	0.873	1.077	<u>39.74</u>

Table 4: The ablation studies on GRID dataset. Base model is trained only with L_1 loss; “+SSIM” means adding structural similarity index loss and “+ADV” means adding adversarial learning to the base model. FID means Fréchet Inception Distance metric. To focus on the frames quality, we provide the ground truth duration for eliminating the interference brought by the discrepancy of predicted length.

We conduct ablation experiments on GRID dataset to analyze the effectiveness of the proposed methods in our work. All the results are shown in Table 4. Experiments show that:

- Adding only SSIM loss obtains the optimal score on PSNR/SSIM/LMD (“+SSIM”);
- Adding only adversarial training causes performance drop on PSNR/SSIM/LMD, which is consistent with previous works [33] (“+ADV”);
- Adding SSIM to model with adversarial training can greatly alleviate the detriment on PSNR/SSIM/LMD brought by adversarial training; make the GAN-based model more stable; obtain the best FID score,

which means the generated lips looks more realistic. (“+SSIM+ADV”).

Previous works [33] claim that 1) PSNR and SSIM cannot well reflect some visual quality *e.g.* resolution; 2) adversarial learning encourages a person to pronounce in diverse ways, leading to diverse lip movements and LMD decrease. Although “+SSIM+ADV” causes marginally PSNR/SSIM/LMD scores losses, “+SSIM+ADV” obtain the best FID score and tends to generate distinct lip images with more realistic texture and local details (*e.g.* wrinkles, beard and teeth). The qualitative results are shown in Figure 6.

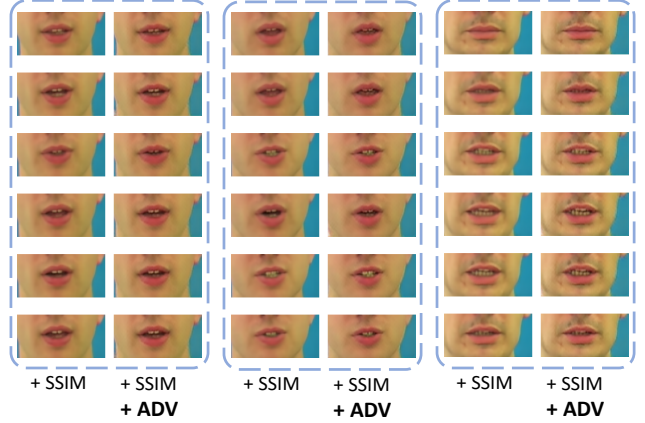


Figure 6: The qualitative evaluation for adversarial learning. It can be clearly seen from the figure that the model with “+ADV” tends to generate more distinct and realistic lip images, especially in the region with wrinkles, beard and teeth.

6. Conclusion

In this work, we point out and analyze the unacceptable inference latency and intractable error propagation existing in AR T2L generation, and propose a novel parallel decoding model HH-T2L to circumvent these problems. Concretely, HH-T2L consists of an identity encoder, a text encoder with duration predictor, a motion decoder and a video decoder. Furthermore, we incorporate the structural similarity index loss and adversarial learning to improve perceptual quality of generated lip frames and alleviate the blurry prediction problem. Extensive experiments conducted on GRID and TCD-TIMIT datasets show that HH-T2L generates lip movements with competitive quality compared with the state-of-the-art AR T2L model DualLip, exceeds the baseline AR model TransformerT2L by a notable margin which is credited to the mitigation of the error propagation problem and exhibits distinct superiority in inference speed, which provides the possibility to bring T2L generation from laboratory to industrial applications.

References

- [1] Ahmed Hussen Abdelaziz, Anushree Prasanna Kumar, Chloe Seivwright, Gabriele Fanelli, Justin Binder, Yannis Stylianou, and Sachin Kajarekar. Audiovisual speech synthesis using tacotron2. *arXiv preprint arXiv:2008.00620*, 2020. **2**
- [2] Triantafyllos Afouras, Joon Son Chung, and Andrew Senior. Deep lip reading: A comparison of models and an online application. In *Proc. Interspeech 2018*, pages 3514–3518, 2018. **5**
- [3] Yannis M Assael, Brendan Shillingford, Shimon Whiteson, and Nando De Freitas. Lipnet: End-to-end sentence-level lipreading. *arXiv preprint arXiv:1611.01599*, 2016. **5**
- [4] Samy Bengio, Oriol Vinyals, Navdeep Jaitly, and Noam Shazeer. Scheduled sampling for sequence prediction with recurrent neural networks. In *Advances in Neural Information Processing Systems*, pages 1171–1179, 2015. **2**
- [5] Lele Chen, Zhiheng Li, Ross K Maddox, Zhiyao Duan, and Chenliang Xu. Lip movements generation at a glance. In *Proceedings of the European Conference on Computer Vision (ECCV)*, pages 520–535, 2018. **2, 5**
- [6] Nanxin Chen, Shinji Watanabe, Jesús Villalba, and Najim Dehak. Non-autoregressive transformer automatic speech recognition. *arXiv preprint arXiv:1911.04908*, 2019. **2, 3**
- [7] Weicong Chen, Xu Tan, Yingce Xia, Tao Qin, Yu Wang, and Tie-Yan Liu. Duallip: A system for joint lip reading and generation. In *Proceedings of the 28th ACM International Conference on Multimedia*, MM ’20, page 1985–1993, New York, NY, USA, 2020. Association for Computing Machinery. **1, 2, 3, 4, 5, 6**
- [8] JS Chung, A Jamaludin, and AP Zisserman. You said that? *British Machine Vision Conference 2017, BMVC 2017*, 2017. **2**
- [9] Joon Son Chung, Andrew Senior, Oriol Vinyals, and Andrew Zisserman. Lip reading sentences in the wild. In *2017 IEEE Conference on Computer Vision and Pattern Recognition (CVPR)*, pages 3444–3453. IEEE, 2017. **5**
- [10] Martin Cooke, Jon Barker, Stuart Cunningham, and Xu Shao. An audio-visual corpus for speech perception and automatic speech recognition. *Journal of the Acoustical Society of America*, 120(5):2421, 2006. **5**
- [11] Chaorui Deng, Ning Ding, Minghui Tan, and Qi Wu. Length-controllable image captioning. *ECCV*, 2020. **2, 3**
- [12] WA Falcon. Pytorch lightning. *GitHub. Note: <https://github.com/PyTorchLightning/pytorch-lightning>*, 3, 2019. **5**
- [13] Bo Fan, Lijuan Wang, Frank K Soong, and Lei Xie. Photo-real talking head with deep bidirectional lstm. In *2015 IEEE International Conference on Acoustics, Speech and Signal Processing (ICASSP)*, pages 4884–4888. IEEE, 2015. **2**
- [14] Ohad Fried, Ayush Tewari, Michael Zollhöfer, Adam Finkelstein, Eli Shechtman, Dan B Goldman, Kyle Genova, Zeyu Jin, Christian Theobalt, and Maneesh Agrawala. Text-based editing of talking-head video. *ACM Transactions on Graphics (TOG)*, 38(4):1–14, 2019. **3**
- [15] Jonas Gehring, Michael Auli, David Grangier, Denis Yarats, and Yann N Dauphin. Convolutional sequence to sequence learning. In *Proceedings of the 34th International Conference on Machine Learning-Volume 70*, pages 1243–1252, 2017. **3**
- [16] Marjan Ghazvininejad, Omer Levy, Yinhan Liu, and Luke Zettlemoyer. Mask-predict: Parallel decoding of conditional masked language models. In *Proceedings of the 2019 Conference on Empirical Methods in Natural Language Processing and the 9th International Joint Conference on Natural Language Processing (EMNLP-IJCNLP)*, pages 6114–6123, 2019. **2, 3**
- [17] Jiatao Gu, James Bradbury, Caiming Xiong, Victor OK Li, and Richard Socher. Non-autoregressive neural machine translation. In *International Conference on Learning Representations*, 2018. **2, 3**
- [18] Naomi Harte and Eoin Gillen. Tcd-timit: An audio-visual corpus of continuous speech. *IEEE Transactions on Multimedia*, 17(5):603–615, 2015. **5**
- [19] Yosuke Higuchi, Shinji Watanabe, Nanxin Chen, Tetsuji Ogawa, and Tetsunori Kobayashi. Mask ctc: Non-autoregressive end-to-end asr with ctc and mask predict. *INTERSPEECH*, 2020. **2, 3**
- [20] Davis E. King. *Dlib-ml: A Machine Learning Toolkit*. JMLR.org, 2009. **5**
- [21] Prajwal KR, Rudrabha Mukhopadhyay, Jerin Philip, Abhishek Jha, Vinay Namboodiri, and CV Jawahar. Towards automatic face-to-face translation. In *Proceedings of the 27th ACM International Conference on Multimedia*, pages 1428–1436, 2019. **3**
- [22] Rithesh Kumar, Jose Sotelo, Kundan Kumar, Alexandre de Brébisson, and Yoshua Bengio. Obamanet: Photo-realistic lip-sync from text. *arXiv preprint arXiv:1801.01442*, 2017. **2, 3**
- [23] Jason Lee, Elman Mansimov, and Kyunghyun Cho. Deterministic non-autoregressive neural sequence modeling by iterative refinement. In *EMNLP*, pages 1173–1182, 2018. **2, 3**
- [24] Jinglin Liu, Yi Ren, Zhou Zhao, Chen Zhang, Baoxing Huai, and Jing Yuan. Fastlr: Non-autoregressive lipreading model with integrate-and-fire. In *Proceedings of the 28th ACM International Conference on Multimedia*, pages 4328–4336, 2020. **2, 3**
- [25] Xuezhe Ma, Chunting Zhou, Xian Li, Graham Neubig, and Eduard Hovy. Flowseq: Non-autoregressive conditional sequence generation with generative flow. In *EMNLP-IJCNLP*, pages 4273–4283, 2019. **2, 3**
- [26] Xudong Mao, Qing Li, Haoran Xie, Raymond YK Lau, Zhen Wang, and Stephen Paul Smolley. Least squares generative adversarial networks. In *Proceedings of the IEEE international conference on computer vision*, pages 2794–2802, 2017. **5**
- [27] Michael Mathieu, Camille Couprie, and Yann LeCun. Deep multi-scale video prediction beyond mean square error. In *4th International Conference on Learning Representations, ICLR 2016*, 2016. **4, 6**
- [28] Chenfeng Miao, Shuang Liang, Minchuan Chen, Jun Ma, Shaojun Wang, and Jing Xiao. Flow-tts: A non-autoregressive network for text to speech based on flow.

- In *ICASSP 2020-2020 IEEE International Conference on Acoustics, Speech and Signal Processing (ICASSP)*, pages 7209–7213. IEEE, 2020. 2, 3
- [29] Kainan Peng, Wei Ping, Zhao Song, and Kexin Zhao. Non-autoregressive neural text-to-speech. *ICML*, 2020. 2, 3
- [30] KR Prajwal, Rudrabha Mukhopadhyay, Vinay P Namboodiri, and CV Jawahar. A lip sync expert is all you need for speech to lip generation in the wild. In *Proceedings of the 28th ACM International Conference on Multimedia*, pages 484–492, 2020. 2
- [31] Yi Ren, Yangjun Ruan, Xu Tan, Tao Qin, Sheng Zhao, Zhou Zhao, and Tie-Yan Liu. FastSpeech: Fast, robust and controllable text to speech. In *Advances in Neural Information Processing Systems*, pages 3165–3174, 2019. 2, 3
- [32] Jonathan Shen, Ruoming Pang, Ron J Weiss, Mike Schuster, Navdeep Jaitly, Zongheng Yang, Zhifeng Chen, Yu Zhang, Yuxuan Wang, Rj Skerrv-Ryan, et al. Natural tts synthesis by conditioning wavenet on mel spectrogram predictions. In *2018 IEEE International Conference on Acoustics, Speech and Signal Processing (ICASSP)*, pages 4779–4783. IEEE, 2018. 6
- [33] Yang Song, Jingwen Zhu, Dawei Li, Andy Wang, and Hairong Qi. Talking face generation by conditional recurrent adversarial network. In *Proceedings of the Twenty-Eighth International Joint Conference on Artificial Intelligence, IJCAI-19*, pages 919–925. International Joint Conferences on Artificial Intelligence Organization, 7 2019. 2, 5, 6, 8
- [34] Ilya Sutskever, Oriol Vinyals, and Quoc V Le. Sequence to sequence learning with neural networks. In *Advances in neural information processing systems*, pages 3104–3112, 2014. 3
- [35] Supasorn Suwajanakorn, Steven M Seitz, and Ira Kemelmacher-Shlizerman. Synthesizing obama: learning lip sync from audio. *ACM Transactions on Graphics (TOG)*, 36(4):1–13, 2017. 2
- [36] Ashish Vaswani, Noam Shazeer, Niki Parmar, Jakob Uszkoreit, Llion Jones, Aidan N Gomez, Łukasz Kaiser, and Illia Polosukhin. Attention is all you need. In *Advances in neural information processing systems*, pages 5998–6008, 2017. 3, 5, 6
- [37] Konstantinos Vougioukas, Stavros Petridis, and Maja Pantic. End-to-end speech-driven realistic facial animation with temporal gans. In *CVPR Workshops*, pages 37–40, 2019. 2
- [38] Michael Wand, Jan Koutník, and Jürgen Schmidhuber. Lipreading with long short-term memory. In *2016 IEEE International Conference on Acoustics, Speech and Signal Processing (ICASSP)*, pages 6115–6119. IEEE, 2016. 5
- [39] Lijuan Wang, Wei Han, Frank K Soong, and Qiang Huo. Text driven 3d photo-realistic talking head. In *Twelfth Annual Conference of the International Speech Communication Association*, 2011. 2
- [40] Zhou Wang. Image quality assessment : From error visibility to structural similarity. *IEEE Transactions on Image Processing*, 2004. 4, 5
- [41] Lijun Wu, Xu Tan, Di He, Fei Tian, Tao Qin, Jianhuang Lai, and Tie-Yan Liu. Beyond error propagation in neural machine translation: Characteristics of language also matter. In *Proceedings of the 2018 Conference on Empirical Methods in Natural Language Processing*, pages 3602–3611, Brussels, Belgium, Oct.-Nov. 2018. Association for Computational Linguistics. 2
- [42] Chengzhu Yu, Heng Lu, Na Hu, Meng Yu, Chao Weng, Kun Xu, Peng Liu, Deyi Tuo, Shiyin Kang, Guangzhi Lei, et al. Durian: Duration informed attention network for multimodal synthesis. *arXiv preprint arXiv:1909.01700*, 2019. 2
- [43] Lingyun Yu, Jun Yu, and Qiang Ling. Mining audio, text and visual information for talking face generation. In *2019 IEEE International Conference on Data Mining (ICDM)*, pages 787–795. IEEE, 2019. 3
- [44] Jiahong Yuan and Mark Liberman. Speaker identification on the scotus corpus. *Journal of the Acoustical Society of America*, 123(5):3878, 2008. 5
- [45] Ruobing Zheng, Zhou Zhu, Bo Song, and Changjiang Ji. Photorealistic lip sync with adversarial temporal convolutional networks. *arXiv preprint arXiv:2002.08700*, 2020. 2
- [46] Hang Zhou, Yu Liu, Ziwei Liu, Ping Luo, and Xiaogang Wang. Talking face generation by adversarially disentangled audio-visual representation. In *Proceedings of the AAAI Conference on Artificial Intelligence*, volume 33, pages 9299–9306, 2019. 2
- [47] Hao Zhu, Huaibo Huang, Yi Li, Aihua Zheng, and Ran He. Arbitrary talking face generation via attentional audio-visual coherence learning. In Christian Bessiere, editor, *Proceedings of the Twenty-Ninth International Joint Conference on Artificial Intelligence, IJCAI-20*, pages 2362–2368. International Joint Conferences on Artificial Intelligence Organization, 7 2020. Main track. 1, 2, 5